研 究 速 報

# Characteristics of GS and SGS Eddies in Homogeneous Isotropic Turbulence

M. Ashraf UDDIN*, Nobuyuki TANIGUCHI*, Mamoru TANAHASHI**,
Toshio MIYAUCHI** and Toshio KOBAYASHI*

## 1. INTRDUCTION

Direct numerical and large-eddy simulations (DNS and LES) have been widely used to study the physics of turbulence. DNS is the exact approach to turbulence simulation but too expensive and is possible only for low Reynolds numbers flow. LES is less expensive and can simulate very complex flow fields in turbulence. With LES method, large-scale motion is directly calculated but small-scale needs to be modeled by subgrid-scale (SGS) models and recent research has been aimed at developing robust SGS models.

It is shown that turbulent flows contain various types of vortical structures and there is a large range of scales. Theorist believed that tube-like structure is a type of eddy, which is the candidate of fine scale structure, particularly, in the small-scale motions in turbulence[1,2,3,4]. In recent studies by direct numerical simulations[5,6,7,8], fine scale tube-like eddies in homogeneous turbulence are observed, and the visualization of this small-scale eddies becomes possible. By direct use of local flow pattern in different flow fields in turbulence, Tanahashi *et al.*[8,9,10,11,12] have shown that the existence of 'coherent fine scale eddies' in turbulence is universal.

Since turbulent flow contains three-dimensional and unsteady structures, more strictly coherent structures but development of SGS model based on coherent structures is relatively scarce. Concerning the structure base SGS model, it seems quite important to know what happened in the filtered field for LES including appearance or disappearance of the tube-like eddies as well as the characteristics of these eddies in resolved or unresolved field.

In the previous study[13], we have identified the GS and SGS eddies in which GS and SGS velocity fields were obtained by filtering DNS velocity field in homogeneous isotropic turbulence for performing *a priori test*. The objective of this study is to investigate the characteristics of these GS and SGS eddies comparing with DNS eddies in homogeneous isotropic turbulence.

*Institute of Industrial Science, the University of Tokyo
**Department of Mechanical and Aerospace Engineering, Tokyo Institute of Technology

## 2. GENERATION OF GS AND SGS VELOCITY FOR LES

### 2.1 DNS Data Base

In this study, DNS data of decaying homogeneous isotropic turbulence has been used, which is conducted by Tanahashi *et al.*[8] and is calculated by using $128^3$ grid points. Reynolds number based on $u_{rms}$ and Taylor microscale, $\lambda$ of the DNS data is $Re_\lambda$ = 64.9.

### 2.2 GS and SGS Velocity Fields

To obtain the grid-scale (GS) and gubgrid-scale (SGS) velocity fields, we have filtered the above DNS velocity field using two classical filters for LES. In LES, a velocity component $u$ can be decomposed into two components, one is called GS component and is denoted by $\bar{u}$, and the other is called SGS component and is denoted by $u'$. Their relation can be expressed as:

$$u = \bar{u} + u' \quad \cdots\cdots (1)$$

The filtered part $\bar{u}$ of the variable $u$ *is* defined by the filtering operation:

$$\bar{u}(x) = \int_D G(x - x', \Delta) u(x') dx', \quad \cdots\cdots (2)$$

in which D is the entire domain, $G$ is filter kernel function and $\Delta$ is the filter width. The dual definition of filtering operation in the Fourier space can be obtained by multiplying the spectrum $\hat{u}(\mathbf{k})$ of $u$(x) by the spectrum $\hat{G}(\mathbf{k})$ of the kernel $G$(x) such that,

$$\hat{\bar{u}}(\mathbf{k}) = \hat{G}(\mathbf{k})\hat{u}(\mathbf{k}), \mathbf{k} = 0, \pm 1, \pm 2, \cdots \quad (3)$$

where $\hat{G}$ is the transfer function associated with the kernel $G$.

In this study, we filter DNS field in Fourier space rather than physical space. For a filter width $\Delta_i$ in i-direction, the filter functions in Fourier space are written as follows:

(I) Gaussian filter:

$$\hat{G}(k_i) = \exp\left\{-\frac{(\Delta_i k_i)^2}{24}\right\} \quad (4)$$

(II) Sharp cutoff filter:

$$\hat{G}(k_i) = \begin{cases} 1, \left(|k_i| \le \frac{\pi}{\Delta_i}\right) \\ 0, \left(|k_i| > \frac{\pi}{\Delta_i}\right) \end{cases} \quad (5)$$

Using these two filters for LES in the Fourier space, one set of DNS data is filtered and the exact GS velocity fields $\bar{u}$ are obtained. After generating $\bar{u}$, the SGS velocity field can be obtained by performing the operation:

$$u' = u - \bar{u} \quad (6)$$

Filter width plays very important role with filter functions in this process. The characteristic filter width $\Delta_i$ is commonly used as the length, approximately proportional to the grid interval $\Delta$ in the previous researches[14,15]. The structures represented by the GS and SGS velocities consequently depend both on the grid interval and on the type of filter employed. In the previous studies[8,9], it is shown that the mean diameter of the coherent fine scale eddy is about 10 times of Kolmogorov microscale ($\eta$) in turbulent flows. Therefore, in this study, the most important filter width, $\Delta_i$ is considered as the length of Kolmogorov microscale in the DNS field with a multiple of 10. Since we are dealing with homogeneous isotropic turbulence, the filter width $\Delta_i$ is same in each direction and hereafter it is denoted by $\bar{\Delta}$, i.e, $\bar{\Delta} = 10\eta$. Although filter width, $\bar{\Delta} = 10\eta$ is a small value, but we have seen that the generation of GS velocity field as well as SGS velocity filed from this $Re_\lambda$ case using this filter width was well possible for both filter functions[13]. Accuracy of this filtering process was also confirmed by comparing the three-dimensional energy spectra for GS as well as SGS velocity fields with DNS velocity field. Detailed of this procedure is reported in our previous studies[13,17,18]. It is also shown that the GS fields for this filter width contribute the large part of energy dissipation rate (about 60%~70%) for all filter functions

## 3. GS AND SGS EDDIES

In order to discuss about GS and SGS eddies, we notice the tube-like coherent eddy by visualization of flows in the DNS field. The concept usually associated with an eddy is that of a region in the flow where the fluid elements are rotating around a 'set of points'. Identification of the eddy or vortex from DNS/LES database is a very difficult and complex task, requiring considerable computational efforts with proper identification method. There are several methods for identification of the vortical structures in turbulence with significant differences[19] and most of them show *threshold* dependence. As we discussed in the introduction, direct 'local flow pattern'[20] can educe coherent structures in several flow fields[8,9,10,11,12], which shows universal characteristics in turbulence. In our previous study[16], using this 'local flow pattern' method we have identified the coherent fine scale eddies and its' axes without using any thresholds and then discussed the spatial distribution of coherent fine scale eddies by visualization of axes in homogeneous isotropic turbulence. In this study, we use the same method to discuss the characteristics GS and SGS eddies in

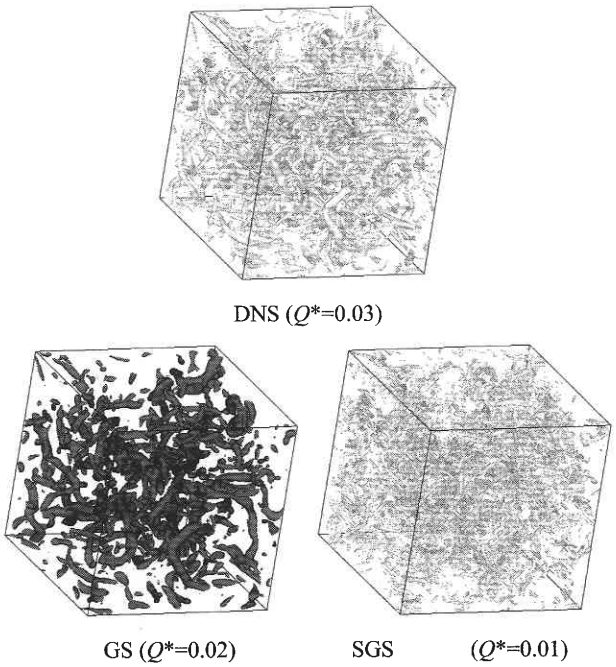


Fig. 1 Contour surfaces of the second invariant of the velocity gradient tensor $Q$ in DNS, GS and SGS fields for $Re_\lambda$ = 64.9. GS and SGS fields are obtained by filtering the DNS field using Sharp cutoff filter. Visualized region is the whole calculation domain. Second invariant is normalized by $\eta$ and $u_{rms}$.

homogeneous isotropic turbulence.

Fig. 1 shows the contour surfaces of normalized second invariant of the velocity gradient tensor $Q$ in DNS as well as GS and SGS fields obtained by using Sharp cutoff filter for $Re_\lambda$ =64.9. The second invariant is defined as follows:

$$Q = -\frac{1}{2}(S_{ij}S_{ij} - W_{ij}W_{ij}), \quad \cdots\cdots (7)$$

where $S_{ij}$ and $W_{ij}$ are the symmetric and antisymmetric part of the velocity gradient tensor $A_{ij}$. In Fig. 1, the visualized region is whole calculation domain and the viewpoint for all cases is same. The level of the isosurface is selected to be $Q$*=0.03 for DNS field, $Q$*=0.02 for GS field and $Q$*=0.01 for SGS fields. Hereafter, * denotes the normalization by Kolmogorov microscale $\eta$ and root mean square of velocity fluctuations, $u_{rms}$ obtained from DNS field. As we discussed above, the visualization of coherent structures depends on the threshold value of $Q$ and we do not concern the strength of the structures, therefore, in this visualization we considered these different values for $Q$ for different fields only to show the vortical structures in different fields by visualization. Fig. 1 clearly indicates that GS and SGS fields contain lots of distinct tube-like eddies somewhat similar to the eddies in the DNS fields, of course different in sizes, which can best be defined as coherent eddies in turbulence[8,9]. It is also clear that the size or length of GS eddies in all cases seems to be larger than SGS eddies. It is known from the classical idea of fluid dynamics that several small-scale structure together form a large-scale structure, i.e., several small (SGS) eddies entirely lie inside a large (GS) eddy in the order of its size. But our DNS database study suggests that the appearance of coherent fine scale eddies in turbulence are quite distinct and unique. The present study also reveals the uniqueness of small-scale and large-scale eddies in turbulent flows. In our previous study[16], we have shown that the tube-like coherent fine scale eddies itself contain its distinct axis as well as local maximum of second invariant on the axis. The present study also suggests that the turbulence fields contain tube-like eddy in different size and length and each eddy has its distinct axis. This result will be worthy to develop a structure base SGS model for LES.

## 4. CHARACTERISTICS OF GS AND SGS EDDIES

### 4.1 Identification method

For visualization of flows in Fig. 1, positive second invariant $Q$ is used and the existence of many tube-like eddies in DNS, GS and SGS fields have shown in homogeneous isotropic turbulence.

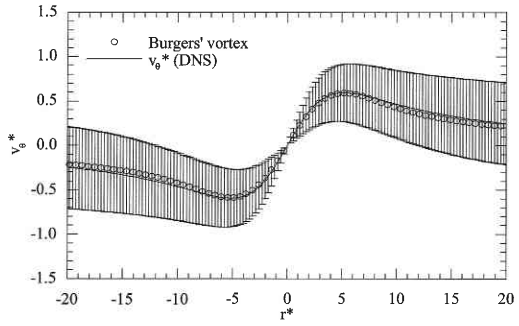


Fig. 2 Mean azimuthal velocity profile of the coherent eddies in the DNS field, normalized by $\eta$ and $u_{rms}$. Symbols represent velocity profile of a Burgers' vortex and error bars denote variances of azimuthal velocity.

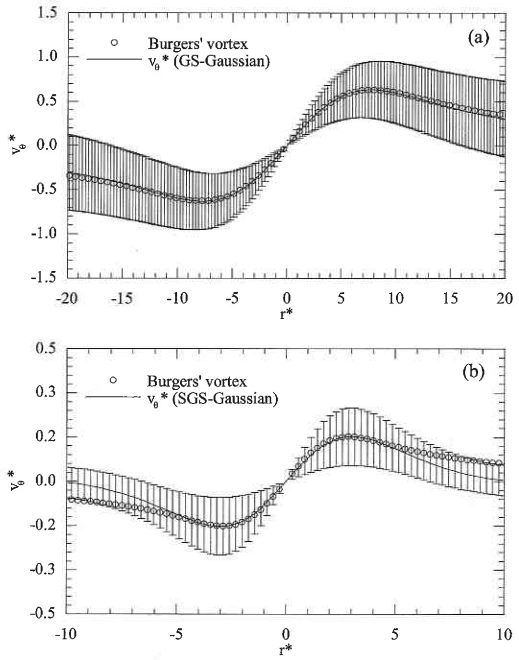


Fig. 3 Same as Fig. 2, but (a) GS field and (b) SGS field obtained by using Gaussian filter.

Obviously these tube-like eddies contain at least one local maximum of $Q$ on its' axis. In this study, using an auto-tracing algorithm the points with local $Q$ maximal on the cross sections of the axis of this eddy are identified and then the statistical properties are calculated around the points. Detailed of this identification method are described in the previous studies [8,9,16].

### 4.2 Statistics of GS and SGS Eddies

Figs. 2–4 show the mean azimuthal velocity profile of tube-like eddies in DNS, GS and SGS fields for two filter functions. In these

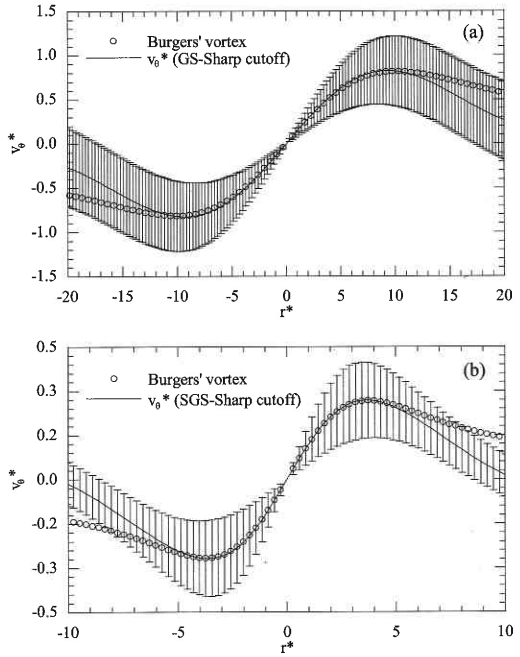


Fig. 4 Same as Fig. 2, but (a) GS field and (b) SGS field obtained by using sharp cutoff filter.

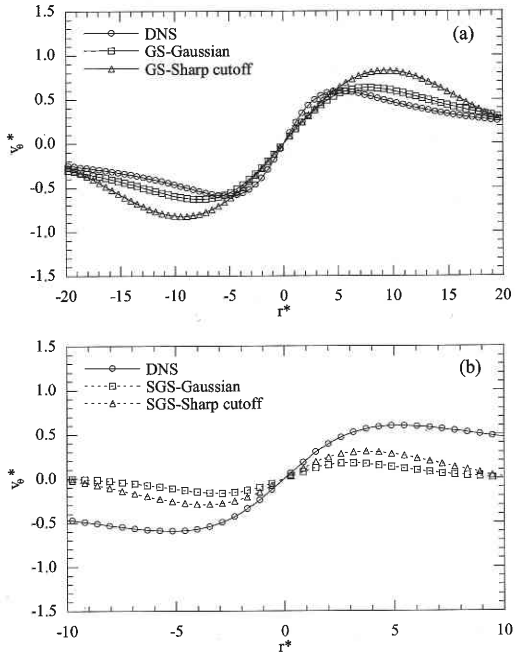


Fig. 5 Comparison of mean azimuthal velocity profile ($v_\theta$) of the DNS, GS and SGS coherent eddies. (a) DNS and GS fields, (b) DNS and SGS fields. In all cases, mean azimuthal velocity profile is normalized by $\eta$ and $u_{rms}$ obtained from the DNS field.

figures, $r$ represents the radius of the eddy, which is determined by the distance between the center and the location where the mean azimuthal velocity reaches the maximum value. Mean azimuthal velocity profiles in all cases are normalized by $u_{rms}$ and $\eta$, which are obtained from the DNS field. In Figs. 2–3, symbols represent an azimuthal velocity of a Burgers' vortex, which is written as follows:

$$v_\theta = \frac{\Gamma}{2\pi r}\left[1 - \exp\left(-\frac{\alpha r^2}{4\nu}\right)\right], \quad \cdots\cdots (8)$$

$$v_z = \alpha z, \quad \cdots\cdots (9)$$

where $\Gamma$ is the circulation of the Burgers' vortex tube and $\alpha$ is a stretching parameter. Using DNS database studies[8,10], it was shown that the mean azimuthal velocity profile of coherent fine scale eddies in homogeneous isotropic turbulence and turbulent mixing layer could be approximated by a Burgers vortex. In these studies, it is also shown that the mean diameter of the coherent fine scale eddies is about $10\eta$ and the maximum of mean azimuthal velocity is about half of $u_{rms}$, and these characteristics of coherent eddies are independent on Reynolds numbers of the flow. Fig. 2 confirms these behaviors of the tube-like coherent eddies for this Reynolds number case. Our interest is to discuss the characteristics of GS and SGS eddies comparing with the DNS results, hence, we have shown approximation of coherent eddies in the GS and SGS fields with that of the Burgers' vortex in Figs. 3–4.

The mean azimuthal velocity profile of GS-Gaussian eddies in Fig. 3(a) shows a good agreement with that of Burgers' vortex in the whole range as it as in DNS field. In Fig. 4(a), the agreement of mean azimuthal velocity profile for GS-sharp cutoff eddies with Burgers' vortex is good for relatively small distance ($r^* < 12\eta$), that is, the Burgers' vortex profile does not collapse with mean azimuthal velocity profile for the large distance. For Gaussian filter, the contribution of GS and SGS velocity fields are obtained from the whole region of DNS velocity field, while sharp cutoff filter separates the DNS velocity field in GS and SGS fields at the cutoff wave number. Maybe, that is one reason of these differences in Fig. 3(a) and 4(a). Moreover, filter size $\bar{\Delta} = 10\eta$ is relatively small. For large filter width, the large-scale structures, i.e., most of the coherent eddies with large diameter accumulate in the GS field. Using large filter width, we have also seen (not shown) that the approximation of mean azimuthal velocity profile by Burgers' vortex becomes quite good for relatively large diameter tube like eddies in GS-sharp cutoff field as well as in GS-gaussian filed. On the other hand, although not in whole range, but Figs. 3(b) and 4(b) also show that the approximation of mean azimuthal velocity pro-

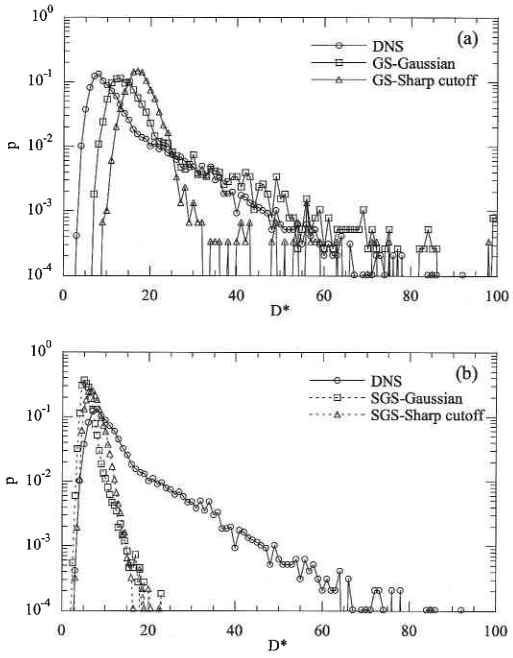


Fig. 6 Probability density function of diameter of coherent eddies normalized by $\eta$. (a) DNS and GS fields, (b) DNS and SGS fields.

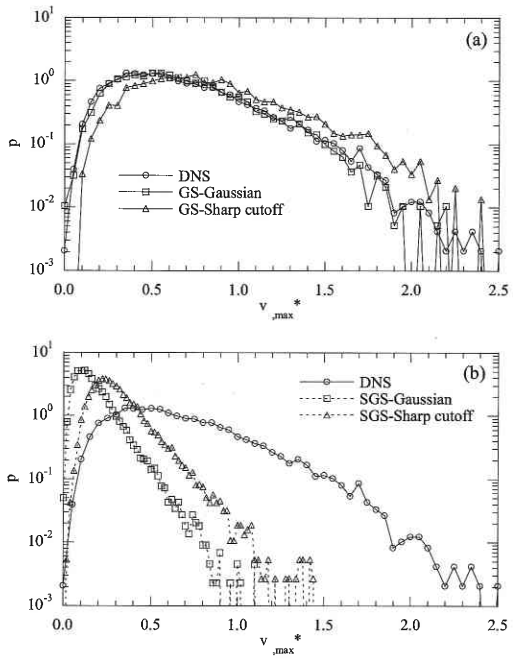


Fig. 7 Probability density function of the maximum of mean azimuthal velocity of coherent eddies normalized by $u_{rms}$. (a) DNS and GS fields, (b) DNS and SGS fields.

file of SGS coherent eddies in both SGS-Gaussian filed and SGS-sharp cutoff field by Burgers' vortex is well in a certain range, and shows almost similar behavior for both filter functions. These results suggest that mean azimuthal velocity profile of coherent structures in LES can be approximate by that of a Burgers' vortex as well as in DNS.

The comparisons of normalized mean azimuthal velocity profile of coherent eddies in DNS, GS and SGS fields for different filter functions are shown in Fig.5. Mean azimuthal velocity profile of GS eddies for different filter functions with this filter width, $\bar{\Delta}$ collapse with DNS profile at $r^*=20\eta$ (Fig. 5(a)). On the other hand, mean azimuthal velocity profile of SGS eddies for different filter functions collapse each other at $r^*=10\eta$ (Fig. 5(b)), but not with DNS profile. In all cases, the maximum of mean azimuthal velocity of GS eddies is higher than DNS eddies, and of SGS eddies is lower than DNS eddies. The maximum of mean azimuthal velocity and diameter of coherent eddies are about $0.6u_{rms}$ and $15\eta$ in GS-Gaussian field, and $0.8u_{rms}$ and $20\eta$ in the GS-sharp cutoff field. On the other hand, the maximum of mean azimuthal velocity and diameter of coherent eddies are about $0.2u_{rms}$ and $5\eta$ in SGS-Gaussian field, and $03u_{rms}$ and $7\eta$ in the SGS-sharp cutoff field. The maximum of mean azimuthal velocity for GS eddies in the Gaussian field is close to the DNS field, but the maximum of mean azimuthal velocity for GS eddies in the sharp cutoff field is larger than the DNS field. In actual LES, GS structures can be identified but SGS structures need to be model by SGS model. Coherent structures have high and thin energy dissipation regions around them and these regions contribute total energy dissipation in turbulence[21]. Since in GS and SGS fields we can see the existence of different kind of coherent eddies somewhat similar to DNS field, which will help us to develop a structures base SGS model for LES.

The probability density functions (pdf) of diameter of tube-like coherent eddies in DNS, GS and SGS fields, which are normalized by $\eta$ are shown in Fig. 6 for different filter functions. It is clear that the peak of pdf of GS eddies in all cases do not coincide with each other or with DNS profile. Moreover, the peak of pdf of GS eddies in the GS-sharp cutoff field shows higher value than in the GS-Gaussian field for this filter width. It is also revealed that the small diameter tube-like coherent eddies in GS field is rare in all cases and large diameter of SGS eddies reaches about $25\eta$. However, the collapse of pdf of diameter in the SGS fields is good, and the peak of pdf for SGS profile increases from the DNS profile for all filter functions.

Fig. 7 shows the pdf of maximum of mean azimuthal velocity of coherent eddies in the same DNS, GS and SGS fields using dif-

ferent filter functions, which is normalized by $u_{rms}$. It is revealed that, GS-Gaussian profile collapse with DNS profile well in the whole range. The profile in the GS-sharp cutoff field is smaller than DNS profile at small azimuthal velocity and larger than that at large azimuthal velocity of the tube-like coherent eddies. The maximum value of mean azimuthal velocity in GS and DNS fields seems to be same. On the other hand, SGS profiles of mean azimuthal velocity for both filter functions do not coincide each other or with DNS profile. The maximum value of mean azimuthal velocity profile is lower than $1.5u_{rms}$, i.e., about half of DNS value. Using large and different filter width, we have seen (not shown) that the pdf of SGS profile becomes very close with DNS profile and the maximum value in the SGS filed never exceeds the maximum value in the DNS field. That is, the characteristics of GS and SGS coherent eddies significantly depend on the filter widths. This behavior is interesting to study on the coherent structure in actual LES or to develop some LES modeling based on the coherent structures in turbulence. In the previous study[8,10], it was shown that the coherent fine scale eddies could be scaled by $\eta$ and *r. m. s* of velocity fluctuations. The above results in the present study also suggest that the GS and SGS coherent structures may possible to scale by $\eta$ and $u_{rms}$ as well as in DNS.

## 5. CONCLUSIONS

DNS velocity field can be separated in GS and SGS velocity field well by using classical filters for LES. Visualization of the contour surfaces of second invariant $Q$ in GS and SGS fields as well as in DNS field, suggests that GS and SGS fields itself contain lots of distinct tube-like eddies, which is considered as GS and SGS eddies in turbulent flow. This study indicates that the DNS field may contain large-scale and small-scale structures together in homogeneous isotropic turbulence. The characteristics of these GS and SGS eddies are somewhat similar to the coherent eddies in DNS fields. These GS and SGS coherent eddies can be scaled by Kolmogorov microscale ($\eta$) and *r.m.s* of velocity fluctuations ($u_{rms}$) as well as in DNS.

This work is supported by the Ministry of Education, Culture, Sports, Science and Technology (Monbu-Kagaku-Sho) under an IT research program "Frontier Simulation Software for Industrial Science".

(Manuscript received, December 2, 2002)

## 6. REFERENCES

1) Townsend, A. A., Proc. R. Soc. Lond., Vol. A208, 534–542 (1951).
2) Tennekes, H., Phys. Fluids, Vol. 11(3), 669–671 (1968).
3) Lundgren, T. S., Phys. Fluids, Vol. 25, 2193–2203 (1982).
4) Pullin, D. I. and Saffman, P. G., Phys. Fluids, A5, 126–145 (1993).
5) She, Z.-S., Jackson, E. and Orszag, S. A., Nature, Vol. 344, 226–228 (1990).
6) Vincent, A. and Meneguzzi, M., J. Fluid Mech., Vol.225, 1–20 (1991).
7) Jimenez, J., Wray, A. A., Saffman, P. G. and Rogallo, R. S., J. Fluid Mech., Vol. 255, 65–90 (1993).
8) Tanahashi, M., Miyauchi, T. and Ikeda, J., Proc. of 11th Symp. on Turbulent Shear Flows, Vol. 1, pp. 4–17–4–22 (1997).
9) Tanahashi, M., Uddin, M. A., Iwase, S. & Miyauchi, T., Trans. JSME, Vol. 65-B (638), 3237–3243 (1999).
10) Tanahashi, M., Miyauchi, T. and Matsuoka, K., Proc. 2nd Int. Symp. on Turbulence, Heat and Mass Transfer, Vol. 2, pp 461–470 (1997).
11) Tanahashi, M., Das, S. K., Shoji, K. and Miyauchi, T., Trans. JSME, Vol. 65–B (638), 3244–3251 (1999).
12) Tanahashi, M., Tsujimoto, T, Karim, M. F., Fujimura, D. and Miyauchi, T., Trans. JSME, Vol. 65–B (640), 3884–3890 (1999).
13) Uddin, M.A., Nobuyuki, T., Tanahashi, M., Miyauchi, T. and Kobayashi, T, 'SEISAN-KENKYU'-Bimonth. J. of IIS, U of Tokyo, Vol. 54, No. 1.2, 30–34, (2002).
14) Piomelli, U., Yu, Y. and Adrian, R. J., Phys. Fluids, Vol. 8(1), 215–224 (1996).
15) Horiuti, K., Phys. Fluids A5 (1), 146–157 (1992).
16) Uddin, M.A., Tanahashi, M., Iwase, S. and Miyauchi, T., 3rd Paci. Symp. on Flow Visualization and Image Processing (PSFVIP-3), Maui, Hawaii, CD-ROM Proc., C3–2 (F3204) (2001).
17) Uddin, M.A., Tanahashi, M., Nobuyuki, T., Iwase, S. and Miyauchi, T., the 4th Int. Conf. on Mech. Eng. (ICME2001), Dhaka, Bangladesh, Vol. II (IV), pp. 81–87, (2001).
18) Uddin, M.A., Nobuyuki, T., Tanahashi, M., Miyauchi, T. and Kobayashi, T, the 15th Symp. on CFD, CD-ROM Proc., LES1, C04–2, Tokyo, Japan, (2001).
19) Jeong, J. and Hussain, F., J. Fluid Mech., 285, 69–94 (1995).
20) Chong, M.S., Perry, A.E. and Cantwell, B.J., Phys. Fluids A2, 765–777 (1990).
21) Tanahashi, M., Miyauchi, T. & Yoshida, T., Transport Phenomena in Thermal Fluid Engineering, Vol. 2, 1256–1261 (1996).